

Cite this article as: Ren Junqiang, Yang Dan, Wang Qi, et al. Effect of Grain Size and Twin Boundary Spacing on Plastic Deformation of Nano-polycrystalline Al Alloy by Molecular Dynamics Study[J]. Rare Metal Materials and Engineering, 2022, 51(07): 2436-2445.

ARTICLE

Effect of Grain Size and Twin Boundary Spacing on Plastic Deformation of Nano-polycrystalline Al Alloy by Molecular Dynamics Study

Ren Junqiang^{1,4}, Yang Dan¹, Wang Qi², Lu Xuefeng¹, Zhang Xudong³, Xue Hongtao¹, Tang Fuling¹, Ding Yutian¹

¹ State Key Laboratory of Advanced Processing and Recycling of Non-ferrous Metals, Lanzhou University of Technology, Lanzhou 730050, China; ² School of Energy Engineering, Huanghuai University, Zhumadian 463000, China; ³ Network Information Center, Xi'an Jiaotong University, Xi'an 710049, China; ⁴ State Key Laboratory for Mechanical Behavior of Materials, Xi'an Jiaotong University, Xi'an 710049, China

Abstract: The molecular dynamics simulations were used to study the effect of grain size and twin density on the plastic deformation of nano-polycrystalline aluminum alloy. The results show that the dislocation density after relaxation is crucial to the microstructure evolution and the inverse Hall-Petch relation of the nano-polycrystalline Al. The staggered tetrahedrons and complex staggered structures are formed in the fine grains, which is attributed to the restriction of grain size. Thus, the auxiliary deformation of grain boundary is activated. The Shockley partial dislocations nucleate and multiply at the grain boundaries when the twin boundary spacing (TBS) is relatively large. However, with decreasing the TBS, the twin boundary becomes the source of the Shockley partial dislocations. A large number of partial dislocation nucleations at the twin boundary will cause the twin boundary to migrate or even disappear. The deformed nano-twins can also be observed during the plastic deformation process. This research provides theoretical basis for the development of advanced nano-polycrystalline Al alloy with adjustable mechanical properties.

Key words: nano-polycrystalline aluminum; grain size; dislocations; twins; molecular dynamics

Due to the excellent mechanical and functional properties, the nanomaterials, as a promising structural material, have attracted widespread attention^[1]. The mechanical properties and deformation of metals and alloys are strongly affected by the grain size (GS), particularly the GS at nanoscale^[2-4]. Hall et al^[5] found that nano-polycrystalline nanomaterials have excellent mechanical properties, such as high strength and high hardness, resulting from the large number of grain boundaries caused by the small GS. It is also found that the strength and hardness of metal materials can be significantly improved by refining the crystal grains into nanoscale, which is 2~10 times smaller than those of the coarse crystal grains^[6-8]. However, when GS is below a certain critical value, the strength is decreased with further decreasing the GS, presenting the inverse Hall-Petch relationship. The process of

controlling the deformation of nano-polycrystalline materials has been investigated^[9-12]. It is generally believed that the intrinsic deformation behavior of nano-polycrystalline materials results from the dynamic interaction between dislocations and grain boundary. However, the specific deformation mechanism is barely studied.

Nanostructures are considered as one of the most effective methods to improve the mechanical properties of material systems^[13]. Kumar et al^[14] studied the deformation mechanism of electrodeposited nano-polycrystalline nickel. Through the observation by in-situ transmission electron microscope (TEM), it is revealed that the dislocation-mediated plasticity is crucial to the deformation of nanocrystalline Ni. The dislocation originates in the grain boundary. The nucleation and movement of complete dislocations become more difficult

Received date: July 08, 2021

Foundation item: Supported by Ministry of Science and Technology of China (2017YFA0700701, 2017YFA0700703); National Natural Science Foundation of China (52061025, 51701189); Sponsored by State Key Laboratory for Mechanical Behavior of Materials (20192104); Joint Fund of Shenyang National Laboratory for Materials Science and State Key Laboratory of Advanced Processing and Recycling of Nonferrous Metals (18LHPY001)

Corresponding author: Ren Junqiang, Ph. D., Assistant Researcher, State Key Laboratory of Advanced Processing and Recycling of Non-ferrous Metals, School of Materials Science and Engineering, Lanzhou University of Technology, Lanzhou 730050, P. R. China, Tel: 0086-931-2976688, E-mail: renjq@lut.edu.cn

Copyright © 2022, Northwest Institute for Nonferrous Metal Research. Published by Science Press. All rights reserved.

with decreasing the GS. Therefore, the dislocations originating in grain boundaries mainly refer to the partial dislocations, such as Shockley partial dislocations. The theoretical model shows that grain boundary slip and grain boundary diffusion in nano-polycrystalline materials can increase the work hardening rate and the tensile plasticity^[15]. Ke et al^[16] observed the grain rotation without dislocation motion in nano-polycrystalline metals. Jin et al^[17] studied the nano-grain films and reported that the grain growth is caused by the grain boundary migration, grain rotation, and grain coalescence. In addition, the grain growth and coalescence induced by the deformation is the main deformation mechanism of bulk metallic materials. Shan et al^[18] suggested that the deformation mechanism is grain boundary diffusion, grain rotation, and other grain boundary deformation mechanisms in in-situ tensile deformation of nano-polycrystalline nickel with GS of 10 nm. Gutkin et al^[19] proposed a theoretical model to explain the deformation mechanism of grain boundary slip and grain rotation in nano-polycrystalline materials. Farkas et al^[20] demonstrated that the grain rotation, grain boundary slip, and grain boundary migration can influence the plastic deformation of metallic nano-polycrystalline bulk materials, according the molecular dynamics (MD) simulation.

The influence of twins on polycrystalline is reported in this study. The strengthening effect is obvious when the twin density is high and the thickness of the twin lamella reaches the nanometer scale^[21-23]. Aluminum is one of the face-centered cubic (fcc) metals with the high stacking fault energy (SFE, ~ 160 mJ/m²). The twins can hardly form during the deformation of coarse-grained metals. Chen et al^[24] observed the stacking faults and twins in nano-polycrystalline Al. Yamakov et al^[25] proved that the mechanical twinning is the main deformation mechanism of nano-polycrystalline Al by MD simulation. The partial dislocation propagation from grain boundaries and the formation of deformation twins are the main deformation mechanisms of nano-polycrystalline materials^[24,26].

The size effect on mechanical properties^[7,8] and deformation mechanism in nano-polycrystalline Al is rarely investigated^[27,28]. Xu et al^[29] used the classical MD simulation to quantify the GS dependence on the mechanical and elastic properties of pure nano-Al specimens and to study the effect of twins on specimens. In this study, the common neighbor analysis (CNA) was used to analyze the crystal defect^[30]. The tensile deformation of nano-polycrystalline Al with different GSs and twin boundary spacings (TBSs) was simulated using MD method. The deformation mechanisms of nano-polycrystalline Al were observed and analyzed by dislocation analysis (DXA) method.

1 Modeling and Methods

MD simulations were performed using the large-scale parallel MD program LAMMPS^[31]. The nano-polycrystalline Al model was generated by the AtomsK^[32] software. The polycrystalline structure with a random distribution of crystal

orientation was constructed through the Voronoi construction method^[33]. The evolution of the atomistic structures was visualized through visualization software Ovito^[34] and Atomeye^[35].

The model was the nano-polycrystalline Al with a constant size of 20 nm×20 nm×20 nm, including 483 143 atoms. Periodic boundary conditions were used in three directions. The nano-polycrystalline Al was deformed under tension along the X direction at the strain rate of 5×10^8 s⁻¹ and a time step of 1.0 fs. The structure was initially relaxed using the steep descent algorithm to obtain an equilibrium state before loading. Additional annealing under zero load was performed for 10 ps by the Nose-Hoover thermostat at 300 K^[36,37]. The isothermal-isobaric ensemble, namely constant atom number, pressure, and temperature (NPT), was applied to keep the system temperature and pressure at 300 K and 0 Pa, respectively. Fig. 1 shows two simulation models established by different softwares. Fig. 1a displays the model with variable grains and average grain sizes (AGSs) without volume change. The AGS of the polycrystalline model is 7.26, 6.49, 5.76, 5.03, 4.57, and 4.24 nm. Fig. 1b displays the model with variable TBS and fixed AGS (5.76 nm). The crystallographic directions were selected as $X=[11\bar{2}]$, $Y=[111]$, and $Z=[\bar{1}10]$. Twins were added along the Y direction and controlled by the number of replications, resulting in different TBSs of 2, 4, 6, 8, 10, and 12 nm.

The embedded atom method (EAM) potentials for Al were employed in the simulation^[38], avoiding the potential dependence on the volume and overcoming the quasi-atom theory restriction caused by the embedded energy. Therefore, EAM potential can better describe the interaction between metal atoms. The total energy of EAM potential can be expressed by Eq.(1), as follows:

$$E_{\text{tot}} = \frac{1}{2} \sum_{ij} \Phi_{ij}(\mathbf{r}_{ij}) + \sum_i F_i(\bar{\rho}_i) \quad (1)$$

where Φ_{ij} is the interaction energy between atoms i and j at positions $\vec{\mathbf{r}}_i$ and $\vec{\mathbf{r}}_j$, respectively; \mathbf{r}_{ij} is the distance between atoms i and j ; F_i is the insertion energy of atom i ; $\bar{\rho}_i$ is the bulk electron density at site $\vec{\mathbf{r}}_i$ induced by all other atoms in the system. Then, $\bar{\rho}_i$ can be expressed by Eq.(2), as follows:

$$\bar{\rho}_i = \sum_{j \neq i} \rho_j(\mathbf{r}_{ij}) \quad (2)$$

The detailed parameters used for calculations are obtained

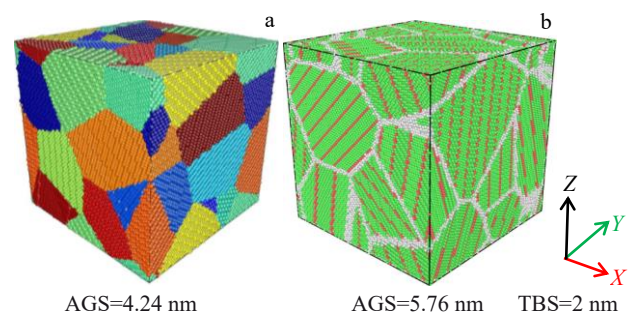


Fig.1 Simulation models of nano-polycrystalline Al by Atomeye (a) and twin content of nano-polycrystalline Al by Ovito (b)

from Ref.[38].

2 Results and Discussion

2.1 Mechanical properties and dislocation density

Fig. 2 shows the tensile stress-strain curves of nano-polycrystalline Al with different AGSs and TBSs. The yield stress is defined as the maximum uniaxial tensile stress. Fig.2a shows that the largest yield stress is 1.65 GPa at the strain of 0.074 when AGS is 5.76 nm. However, the stress usually has a slight decrease before reaching the maximum value with different TBSs, as shown in Fig.2b. The largest yield stress is 1.6 GPa at the strain of 0.074 when AGS=5.76 nm with TBS= 10 nm.

Fig. 3a shows the yield stress as a function of GS. S indicates the slope of the fitting line. The nano-polycrystalline Al with AGS=5.76 nm shows the yield stress of 1.65 GPa, and it declines to 1.47 GPa with AGS=7.26 nm, indicating that the classic Hall-Petch relationship can be observed between the yield stress and AGS when AGS is larger than the critical GS of 5.76 nm. However, when AGS is less than 5.76 nm, the yield stress is continuously decreased with decreasing the AGS, suggesting that the inverse Hall-Petch relationship^[39,40] dominates the influence mechanism. The flow stress can be obtained by the average stress at the statistical strains from 0.15 to 0.30. Fig.3a shows that the flow stress changes with GS under tensile loads, which is similar to the variation trend of yield stress. The yield stress σ_y ^[39,40] can be fitted according to Eq.(3), as follows:

$$\sigma_y \approx kd^{-\frac{1}{2}} \tag{3}$$

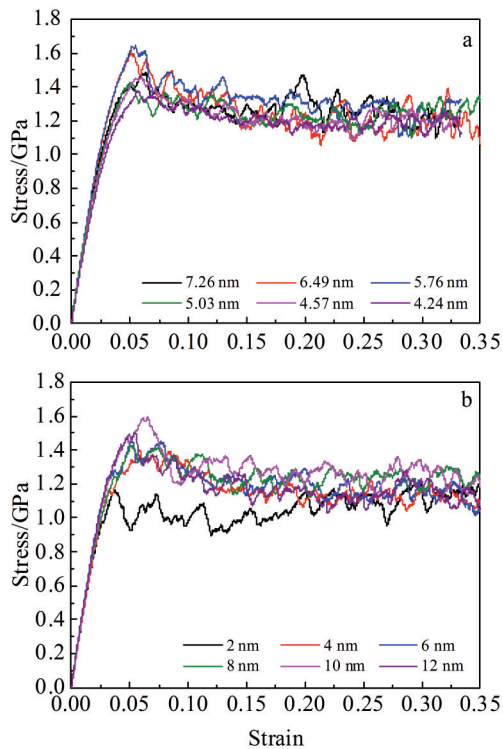


Fig.2 Stress-strain curves of nano-polycrystalline Al with different AGSs (a) and TBSs (b)

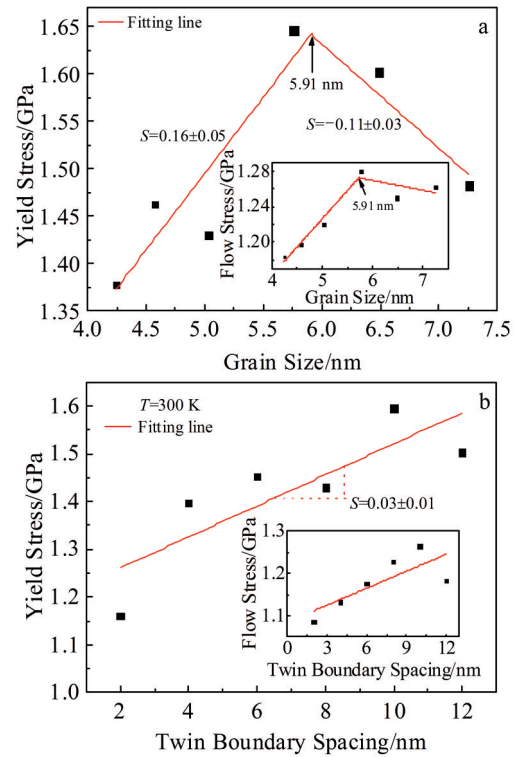


Fig.3 Relationship of yield stress with GS (a) and TBS (b) of nano-polycrystalline Al

where d is GS or TBS and k is a constant.

The linear fitting results show that the critical GS for the inverse Hall-Petch relationship is 5.91 nm, which is consistent with the results in Ref.[41,42]. By changing the twin density in nano-polycrystalline Al, the yield stress is increased with increasing TBS, as shown in Fig.3b. The linear fitting results show that the relationships of yield stress with GS and TBS are both linear. The absolute value of the slope between yield stress and GS is 0.16 ± 0.05 and 0.11 ± 0.03 at the increasing and decreasing stages of yield stress, respectively, which is larger than that between yield stress and TBS (0.03 ± 0.01), indicating that the effect of GS on the yield stress is greater than that of TBS.

The relationship between dislocation density and strain at different GSs and TBSs is shown in Fig. 4. The dislocation density is the ratio of the dislocation line to the volume. The smaller the GS, the higher the initial dislocation density after relaxation at 300 K due to the larger grain boundary volume ratio, and the easier the dislocation nucleation at the grain boundary. The dislocation density is decreased with increasing the twin density and strain.

2.2 Microstructure evolution and plasticity mechanism

The evolution of dislocation and stacking faults of nano-polycrystalline Al under yield stress was observed by DXA method. The main dislocation structure is Shockley partial dislocation, followed by perfect dislocation, whereas other types of dislocations account for a small amount. The Shockley partial dislocation deformation is the main plastic

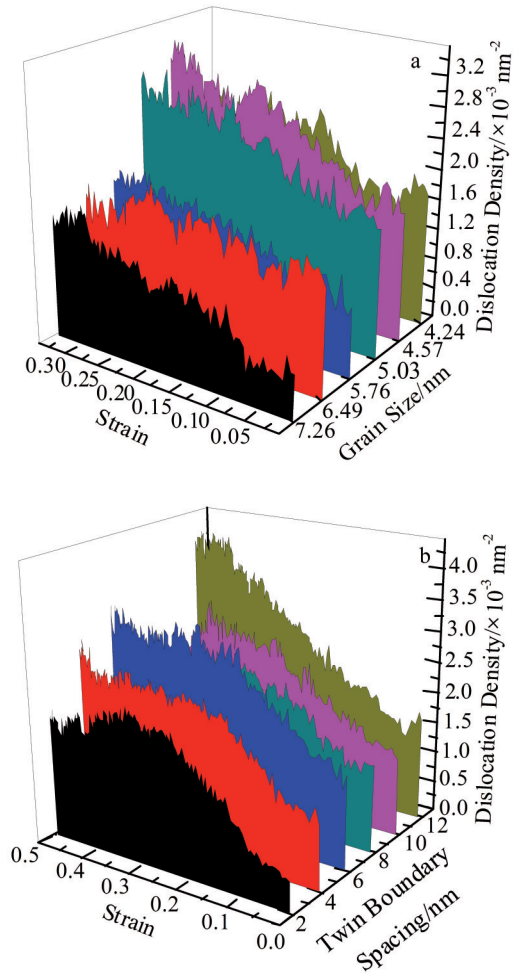


Fig.4 Influences of GS (a) and TBS (b) on dislocation density and strain of nano-polycrystalline Al

deformation mechanism of the nano-polycrystalline Al. The dislocations are nucleated and propagated from the grain boundary, as shown in Fig. 5. Fig. 5a~5f show the stacking

faults and grain boundaries, and Fig. 5g~5l show the dislocations. Red and gray atoms represent the ones of close-packed hexagonal (hcp) structures and grain boundaries, respectively; the blue, green, rose red, yellow, and light blue lines represent the perfect dislocation, Shockley dislocation, stair-rod dislocation, Hirth dislocation, and Frank dislocation, respectively; the black arrows show that the stacking faults follow the leading partial dislocations and then are propagated from the grain boundaries. The space of dislocation motion is decreased with decreasing the GS, leading to high dislocation density, easy dislocation tangle, and the formation of dislocation cell or dislocation wall^[5]. The yield stress and GS show an inverse Hall-Petch relationship when AGS is less than 5.76 nm, which is related to the dislocation density at the end of model relaxation, as shown in Fig. 3a and Fig. 4a. The nucleation and multiplication of dislocations at grain boundaries lead to the decrease in yield stress and the slight deformation. When GS is larger, the dislocation line is short and messy. When GS increases to 7.26 nm, the deformation of nano-twins can be observed, as shown in Fig. 6. Yield stress and GS show a classical Hall-Petch relationship when GS is larger than the critical size (5.91 nm), which is consistent with the classical dislocation-mediated deformation mechanism.

The grain boundaries in the bulk polycrystalline materials are obstacles to dislocation movement. The yield strength of polycrystalline metals is increased with decreasing the obstacle distance, presenting the classical Hall-Petch relationship^[39,40,43]. When the crystallite size is 20~40 nm, the grains can hardly accommodate more dislocations, which involves the plastic deformation mechanisms, such as grain boundary sliding, partial dislocation propagation, and grain boundary absorption^[25,44]. With further reducing the crystallite size to <20 nm, the inverse Hall-Petch relationship dominates instead of the Hall-Petch relationship. The yield strength is weakened with decreasing the GS, when the grain boundary auxiliary deformation is activated.

When GS reduces to several nanometers, the Hall-Petch

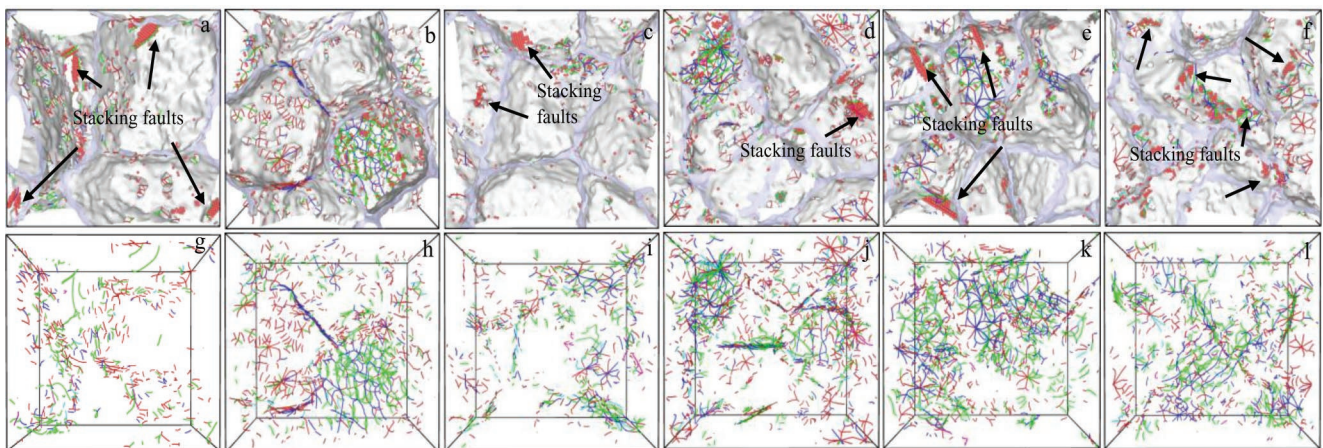


Fig.5 Stacking faults with grain boundaries (a~f) and dislocation lines (g~l) of nano-polycrystalline Al with different AGSs at different strains: (a, g) AGS=7.26 nm, $\varepsilon=0.070$; (b, h) AGS=6.49 nm, $\varepsilon=0.060$; (c, i) AGS=5.76 nm, $\varepsilon=0.060$; (d, j) AGS=5.03 nm, $\varepsilon=0.061$; (e, k) AGS=4.57 nm, $\varepsilon=0.069$; (f, l) AGS=4.24 nm, $\varepsilon=0.067$

relationship will not be considered in discussion. In this research, when the GS decreases, a large number of dislocations nucleate at the nanocrystalline boundaries and form the dislocation tangles after relaxation, resulting in the increase in dislocation density and grain boundary energy. When the GS is less than the critical size for stable pile up of dislocations, i.e., when the AGS of nano-polycrystalline Al is less than 5.91 nm, the piling-up of dislocations is not stable. The partial dislocation is initiated under the external stress, and the yield stress decreases. The inverse Hall-Petch relationship exists between the yield stress and GS, inferring a grain boundary softening behavior, and even the grain sliding or rotation.

The main plastic deformation mechanism of nano-polycrystalline Al is the nucleation and propagation of Shockley partial dislocation at the grain boundary. The stacking fault is formed in grains after the motion of Shockley partial dislocation, as indicated by the red atoms in Fig.6. The crystallographic orientation of grains is random, and the Schmitt factors are different under uniaxial tensile stress along different directions, leading to the uneven distribution of dislocations in grains. Dislocation tangles in grains of small GS easily occur with increasing the strain due to the space restriction of dislocation motion, as shown in the black-dash areas in Fig.6. It can be seen that even in nano-polycrystalline Al with larger AGS (7.26 nm), the grains are still small and restrict the dislocation motion. However, in the large grains, the nano-twins can be observed. The nano-twins caused by stacking faults are not stable and usually disappear under stress, as shown in the black-dash area in Fig. 6b. There are two types of stacking faults: intrinsic stacking fault (ISF) and extrinsic stacking fault (ESF) on the $\{111\}$ slip plane. For example, two adjacent hcp lines indicate the ISF, and one hcp-coordinated atom represents the ESF. When the Shockley partial dislocations of two extended dislocations on

neighboring planes glide over each other, the ISFs of the two dislocations in the overlap region combine to form the ESF. With increasing the plastic strain, the process leads to the formation of nano-twins^[45].

In addition to the stacking faults formed by extended dislocation, the Lomer-Cottrell lock and stacking fault tetrahedron are important factors of plastic deformation mechanisms in nanocrystals. The cross-slip of two Shockley partial dislocations occurs on their glide planes, forming a Lomer-Cottrell lock, such as the $(11\bar{1})$ and (111) glide planes in Fig. 7a^[26,46]. The Frank dislocations decompose into low energy stair-rod dislocations and Shockley dislocations on the intersecting slip plane, according to the reaction type. The dislocation reaction can be expressed as follows:

$$\frac{1}{3} \langle 111 \rangle \rightarrow \frac{1}{6} \langle 112 \rangle + \frac{1}{6} \langle 110 \rangle \quad (4)$$

The stacking fault tetrahedral structures are generated inside the grains^[47], as shown in Fig. 7b, which are mainly formed by the stair-rod dislocations under tensile loading. These structures will merge to form the stable stacking faults structure, as shown in Fig. 7b. With decreasing the GS, the number of stacking fault tetrahedral structures formed in the crystal grain is increased, and the structure is transformed into a more complex structure. These defects act as a barrier against the dislocation motion on the glide planes, affecting the strain hardening and fracture of the nanocrystal materials.

The dislocation tangle is a special dislocation array, which is formed during the plastic deformation. Thus, the grain boundary is regarded as a dislocation source to propagate several dislocations in different slip planes, including the perfect dislocation, Shockley dislocation, stair-rod dislocation, Hirth dislocation, Frank dislocation, and others dislocations. Eventually, these dislocations meet the barrier, and the expansion of the dislocations is restricted. However, these different types of dislocations are entangled at one point,

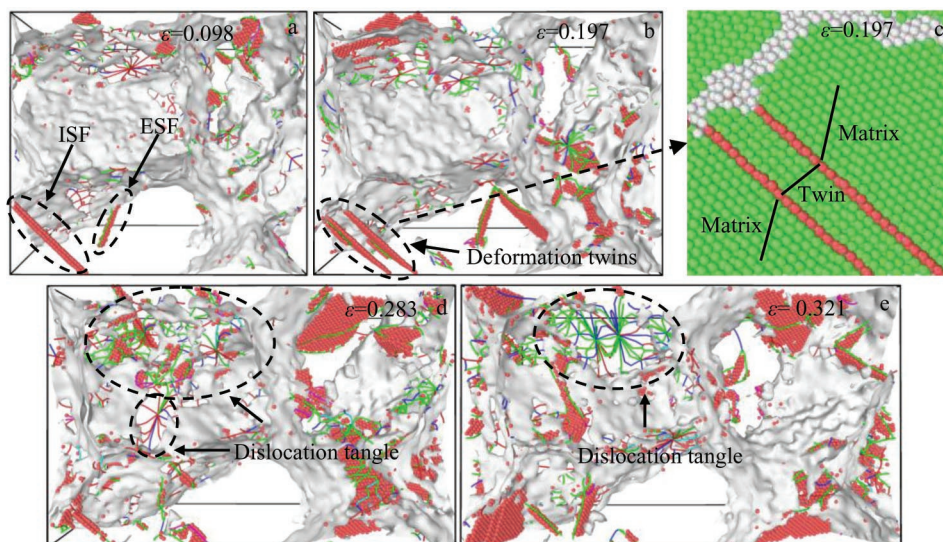


Fig.6 Formation of dislocation tangles and twins in nano-polycrystalline Al during plastic deformation with AGS=7.26 nm at different strains: (a) $\epsilon=0.098$, (b, c) $\epsilon=0.197$, (d) $\epsilon=0.283$, and (e) $\epsilon=0.321$

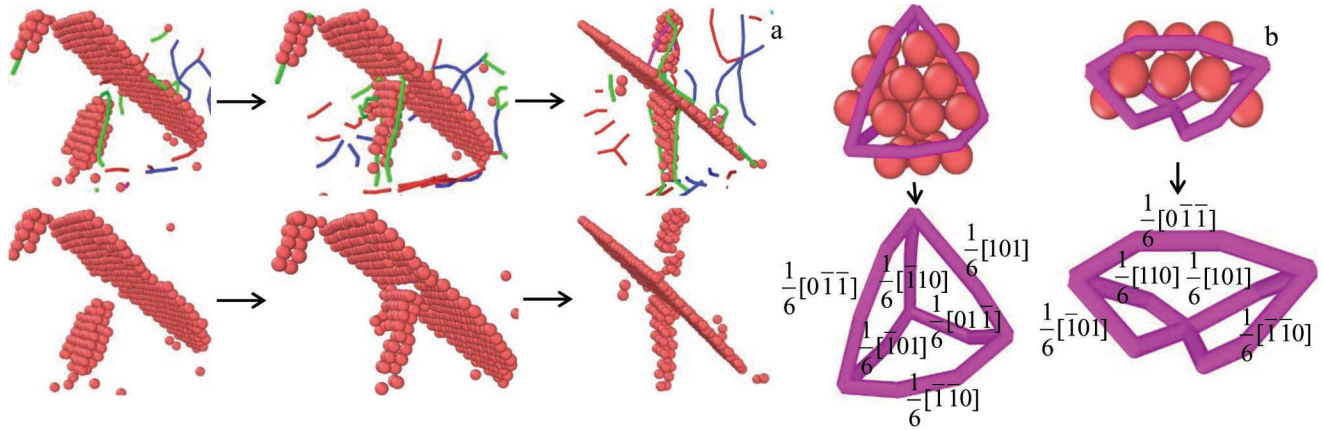


Fig.7 Formation of Lomer-Cottrell lock (a) and stacking fault tetrahedron structures (b) in nano-polycrystalline Al with AGS=6.49 nm

instead of combining with each other. With increasing the plastic strain, the dislocation content in the grains is increased rapidly due to the increasing nucleation activity at grain boundaries under the constant tensile load^[12]. The dislocation density at the dislocation entanglement area increases obviously, and a large number of extended dislocations are also formed in the large grains. During the large plastic deformation, the grain boundaries in nanocrystals glide or rotate slightly. The dislocation entanglement points near the grain boundaries are subjected to large shear stress, and the space of dislocation motion and the elastic interaction between dislocations are changed. The dislocation breaks through the entanglement and continues to move on the glide plane, and then the dislocation entanglement is finally released, as shown in the dashed circle areas in Fig. 8. The extended dislocations are another major influence factor of plastic deformation. The red atoms in Fig. 8 represent the extended dislocations, which are firstly increased and then decreased with increasing the strain. For example, the leading

Shockley partial dislocations with the Burger vector of $\frac{1}{6}[\bar{1}21]$ nucleate firstly from the grain boundaries and grain junctions when the stress exceeds the threshold. Then, the terminal part of Shockley partial dislocations with Burger vector of $\frac{1}{6}[\bar{2}1\bar{1}]$ following the leading one is connected by the stacking faults. Finally, the leading and terminal parts of Shockley partial dislocations react with each other to form full dislocations. The stacking fault tetrahedrons remain after the extended dislocation reaction in the nanocrystals, as shown in Fig.8f. The dislocation process can be expressed as follows:

$$\frac{1}{6}[\bar{1}21] + \frac{1}{6}[\bar{2}1\bar{1}] = \frac{1}{2}[\bar{1}10] \quad (5)$$

The deformation mechanism of conventional coarse-grained materials is mainly the dislocation and dislocation interactions with crystal defects, impurity atoms, and the secondary phase particles. However, numerous grain boundaries can hinder the dislocation slip in coarse-grained materials, leading to the plastic deformation^[47]. The joints of

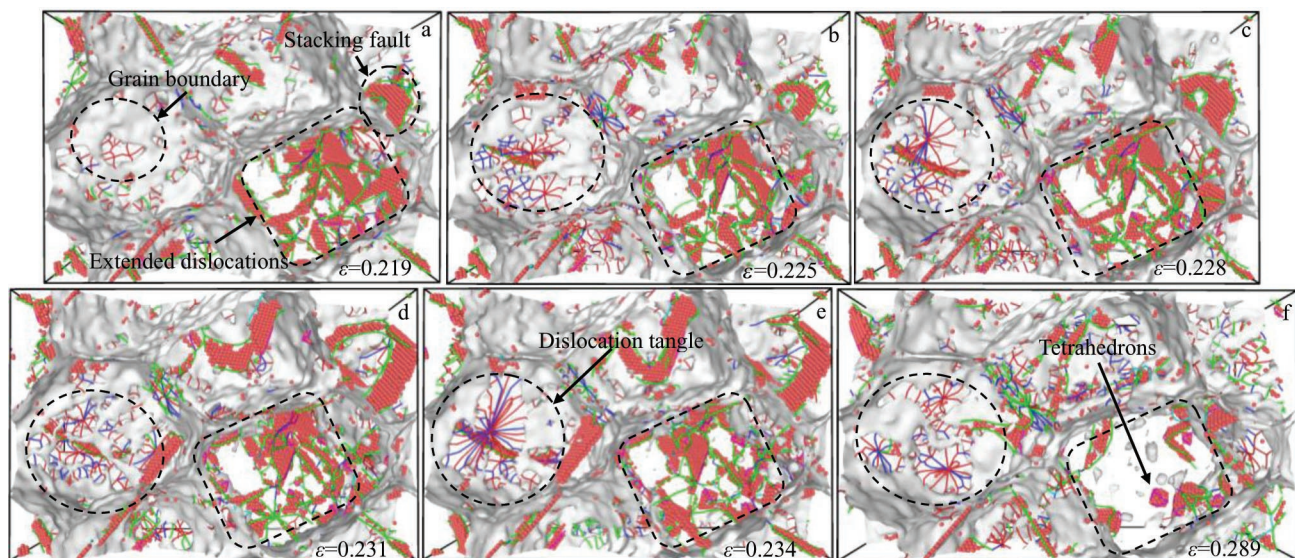


Fig.8 Evolution of dislocation entanglement and stacking faults in nano-polycrystalline Al with AGS=6.49 nm at different strains: (a) $\varepsilon=0.219$; (b) $\varepsilon=0.225$; (c) $\varepsilon=0.228$; (d) $\varepsilon=0.231$; (e) $\varepsilon=0.234$; (f) $\varepsilon=0.289$

grain boundaries are critical to the grain growth, merging, and new grain formation. As shown in the dashed circle areas in Fig. 9a₁, 9c₂, and 9f₁, when a joint contains more than three grain boundaries, the joint becomes unstable and easy to decompose under stress. Fig. 9a₁~9a₃ and 9f₁~9f₃ show the decomposition and merging of grain boundaries with increasing the strain. The new grain G6 is formed at the joint of four grain boundaries, surrounded by grains G1~G5, as shown in Fig. 9c₃. Gutkin et al.^[19] proposed a theoretical model to explain the deformation mechanism of grain boundary slip and grain rotation in nano-polycrystalline materials. The intergranular dislocations react with each other at the trigeminal grain boundaries^[48], indicating the decomposition of grain boundary dislocation, which destroys the balance among the grain boundary dislocations. Therefore, the joint of the triple junction hinders the sliding of the grain boundary. As shown in Fig. 9b₁~9b₃, the equiaxed grain with a triple

junction is relatively stable. The grain profile of the dashed area is quadrilateral at the strain of 0.008, as shown in Fig. 9d₁. The grain becomes hexagonal at the strain of 0.203. The grain rotates under tensile stress. Then, the grain boundary migration, grain rotation, and grain consolidation are the main deformation mechanisms of bulk metallic nanopolycrystalline materials^[49]. Fig. 9e₂ and 9e₃ show that the twin deformation occurs during the plastic deformation of nanopolycrystalline Al.

The twins with different TBSs in the nanocrystals are considered to investigate the effects of TBS on the mechanical characteristics and deformation mechanisms of nanopolycrystalline Al. Fig. 10a shows the nano-polycrystalline Al model with TBS=2 nm. The Atomeye visualization software was used, and the dark blue, light blue, and red atoms in Fig. 10 represent fcc, hcp, and disordered atoms, respectively. With the tensile deformation proceeding, the partial

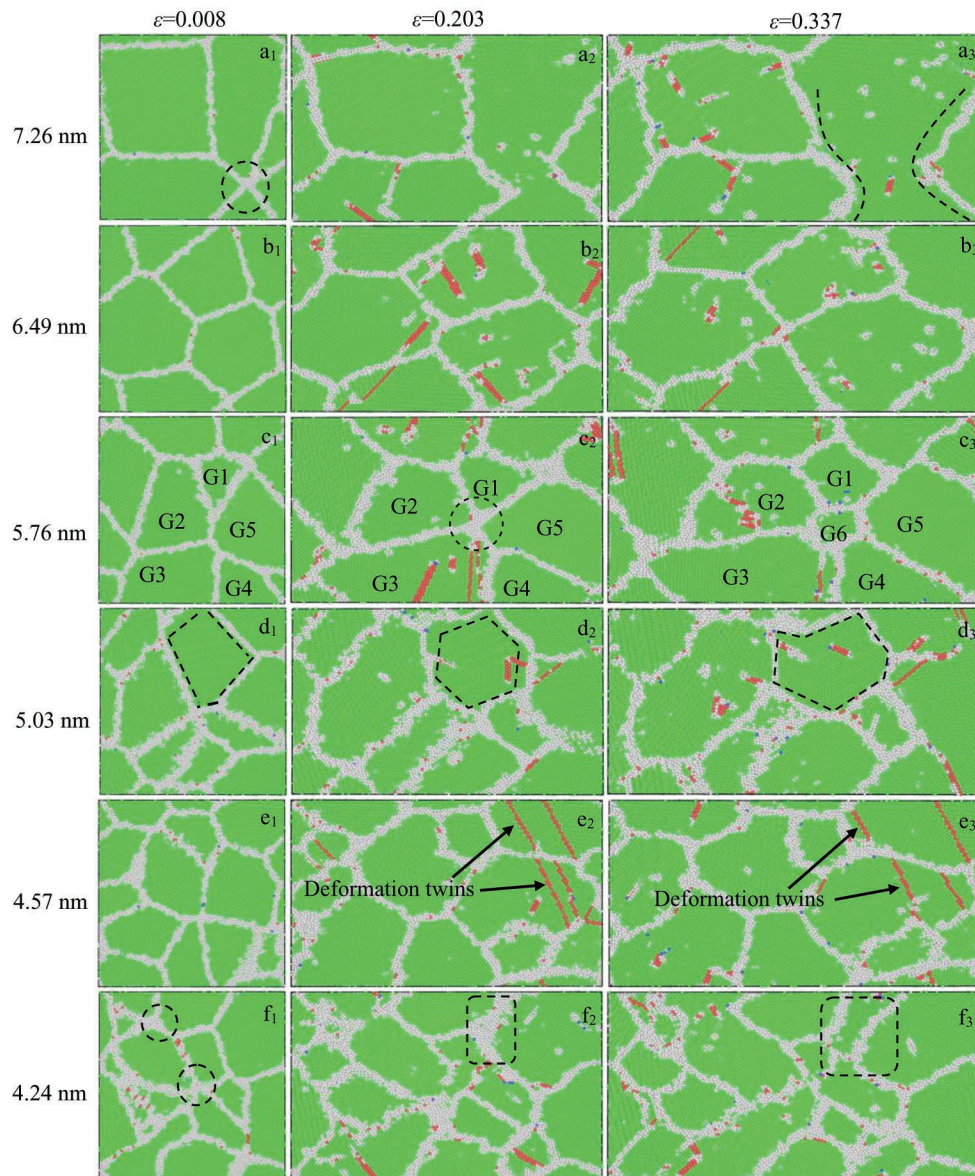


Fig.9 Evolution of recrystallization and grain growth in nano-polycrystalline Al with different AGSs under different strains

dislocation nucleation and motion from the grain boundary and twin boundary are major deformation modes in the nano-polycrystalline Al due to the lack of dislocation sources in the grains. As shown in Fig. 10b, the plasticity of nano-polycrystalline Al is caused by partial dislocations at grain boundaries or twin boundaries, leading to the migration of twin boundaries and even disappearance of twins in grain G2 during deformation. The partial dislocation nucleates at the intersection of the twin boundary, and the grain boundary expands along the twin boundary. The stacking fault causes the migration of the twin boundary and is eventually absorbed by grain boundaries. This process also promotes the migration of the grain boundaries. Fig. 10a~10c show the twin boundary changes inside G3 and G4 grains. The G4 and G6 grains combine to form the new grain G46, as shown in Fig. 10a~10d. The new deformation twins are generated and then

disappear in the grains under large tensile loading, as shown in Fig. 10e and 10f. Besides, the size and morphology of multiple-twinned nano-polycrystalline grains are changed during the deformation process.

Fig. 11a shows the nano-polycrystalline Al model with TBS=10 nm. The grains merge into the new grains with increasing the strain. The G1 and G5 grains merge to form the new grain G15, as shown in Fig. 11a and 11b. The newly formed grain boundary between the grain G4 and the new grain G6 originates from the nucleation and movement of dislocations in grains. As shown in Fig. 11c, the red atomic plane represents the twin boundary, and the green line (partial dislocation line) indicates that the dislocation nucleation occurs at the twin boundary. The dislocation interaction in the twin boundary destroys the twin boundary. Due to the twin boundary migration and the dislocation absorption of grain boundary,

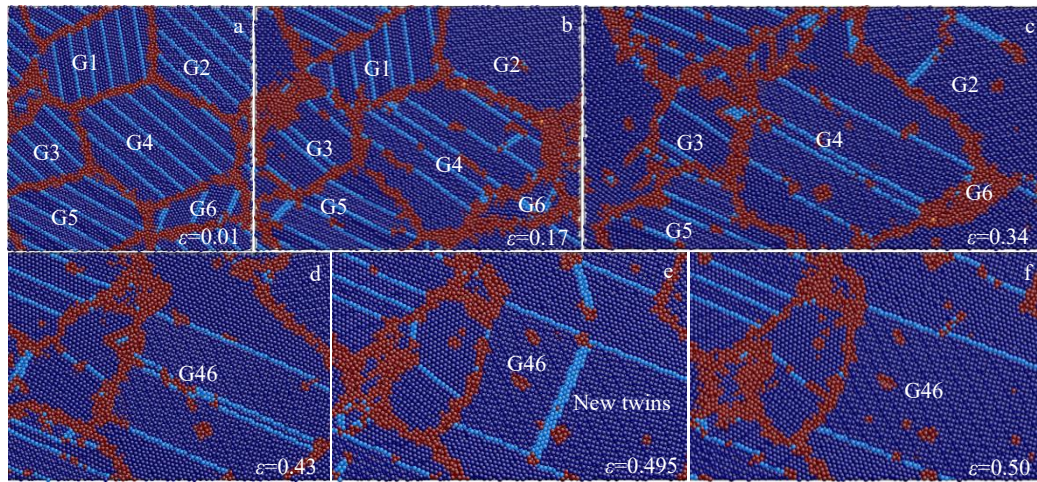


Fig. 10 Atomic configurations of nano-polycrystalline Al with TBS=2 nm at 300 K and different strains: (a) $\varepsilon=0.01$, (b) $\varepsilon=0.17$, (c) $\varepsilon=0.34$, (d) $\varepsilon=0.43$, (e) $\varepsilon=0.495$, and (f) $\varepsilon=0.50$

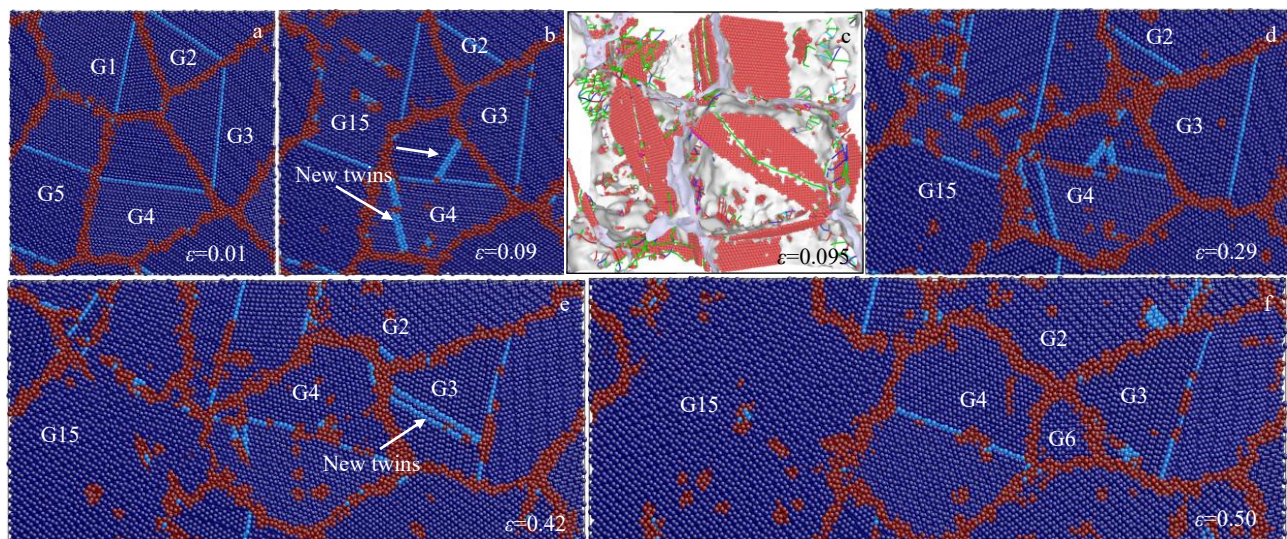


Fig. 11 Atomic configurations of nano-polycrystalline Al with TBS=10 nm at 300 K and different strains: (a) $\varepsilon=0.01$, (b) $\varepsilon=0.09$, (c) $\varepsilon=0.095$, (d) $\varepsilon=0.29$, (e) $\varepsilon=0.42$, and (f) $\varepsilon=0.50$

the original straight grain boundary becomes disordered and curved. The dislocation nucleation mainly occurs at grain boundary of nano-polycrystalline Al with large TBS. Deformation twins can also be observed in the plastic deformation of nano-polycrystalline Al with large TBS. The grains with large TBS have a better dislocation storage ability than those with small TBS do^[50]. The storage ability of dislocations strongly influences the dislocation density and tensile stress. If TBS of the nano-polycrystalline Al is too small for dislocation pile-up, the mechanical properties are restricted. As shown in Fig. 4b and Fig. 3b, the nano-polycrystalline Al with large TBS has high dislocation density and high yield stress. Combined with the analyses of the deformation mechanism based on Fig. 9~Fig. 11, in the early deformation, the plastic deformation is mainly controlled by the partial dislocation behavior, such as the reaction between the dislocations, the formation of the stacking fault tetrahedral structure, and the formation of deformation twins. However, with increasing the strain, the plastic deformation is mainly controlled by the grain boundary behavior, such as grain growth, merging, and new grain formation.

3 Conclusions

1) When the average grain size (AGS) is below 5.91 nm, the inverse Hall-Petch mechanism dominates the relationship between the grain size and the yield stress. As a result, the dislocation density of grain boundary is increased with decreasing the AGS, thereby leading to the activation of grain boundary auxiliary deformation.

2) During the plastic deformation, the grain boundaries are prone to decomposition and merging to form new grains or to facilitate the grain growth. The triple junction is relatively stable. The dislocations movement is restricted by twin boundary spacing (TBS), therefore forming dislocation tangles inside the fine grains. The stacking fault tetrahedron structures generated in the grains are increased with decreasing AGS, and they evolve into a more complex staggered structure. The unstable nano-twins caused by intrinsic stacking fault can be observed.

3) The yield stress is decreased with decreasing TBS. TBS is crucial to determine the mechanical properties of nano-twinned Al. The yield stress of nano-twinned Al is associated with the dislocation nucleation at grain boundaries and twin boundaries. Some twin boundaries migrate during the plastic deformation and are absorbed by grain boundaries.

References

- 1 Kumar K S, Swygenhoven H V, Suresh S. *Acta Materialia*[J], 2003, 51(19): 5743
- 2 Schiøtz J, Di Tolla F D, Jacobsen K W. *Nature*[J], 1998, 391(6667): 561
- 3 Zhang Y F, Luo X B, Li C et al. *Rare Metal Materials and Engineering*[J], 2020, 49(12): 4097
- 4 Zhang Xingli, Sun Zhaowei, Kong Xianren et al. *Rare Metal Materials and Engineering*[J], 2010, 39(5): 853 (in Chinese)
- 5 Hall E O. *Proceedings of the Physical Society: Section B*[J], 1951, 64(9): 742
- 6 Bulatov V, Abraham F F, Kubin L et al. *Nature*[J], 1998, 391(6668): 669
- 7 Jeong G, Park J, Nam S et al. *Archives of Metallurgy and Materials*[J], 2015, 60(2B): 1287
- 8 Choi H J, Lee S W, Park J S et al. *Materials Transactions*[J], 2009, 50(3): 640
- 9 Birringer R, Gleiter H, Klein H P et al. *Physics Letters A*[J], 1984, 102(8): 365
- 10 Karch J, Birringer R, Gleiter H. *Nature*[J], 1987, 330(6148): 556
- 11 Nastasi M, Parkin D M, Gleiter H. *Mechanical Properties and Deformation Behavior of Materials Having Ultra-Fine Microstructures*[M]. Berlin: Springer Science & Business Media, 1993
- 12 Siegel R W. *Materials Science Forum*[J], 1997, 235-238: 851
- 13 Cavaliere P. *Handbook of Mechanical Nanostructuring*[M]. New York: John Wiley & Sons, 2015
- 14 Kumar K S, Suresh S, Chisholm M F et al. *Acta Materialia*[J], 2003, 51(2): 387
- 15 Ovid'ko I A, Sheinerman A G. *Acta Materialia*[J], 2009, 57(7): 2217
- 16 Ke M, Hackney S A, Milligan W W et al. *Nanostructured Materials*[J], 1995, 5(6): 689
- 17 Jin M, Minor A M, Stach E A et al. *Acta Materialia*[J], 2004, 52(18): 5381
- 18 Shan Z W, Stach E A, Jmk W et al. *Science*[J], 2004, 305(5684): 654
- 19 Gutkin M Y, Ovid'ko I A, Skiba N V. *Acta Materialia*[J], 2003, 51(14): 4059
- 20 Farkas D, Mohanty S, Monk J. *Materials Science and Engineering A*[J], 2008, 493(1-2): 33
- 21 Lu L, Shen Y F, Chen X H et al. *Science*[J], 2004, 304(5669): 422
- 22 Luo Dechun, Rui Zhiyuan, Fu Rong et al. *Rare Metal Materials and Engineering*[J], 2017, 46(12): 3792 (in Chinese)
- 23 Zhang Xiaoyong, Zhang Bin, Li Chao et al. *Rare Metal Materials and Engineering*[J], 2013, 42(10): 2057 (in Chinese)
- 24 Chen M W, Ma E, Hemker K J et al. *Science*[J], 2003, 300(5623): 1275
- 25 Yamakov V, Wolf D, Phillpot S R et al. *Nature Materials*[J], 2004, 3(1): 43
- 26 Zhu Y T, Langdon T G. *Materials Science and Engineering A*[J], 2005, 409(1-2): 234
- 27 Kadau K, Lomdahl P S, Holian B L et al. *Metallurgical and Materials Transactions A*[J], 2004, 35(9): 2719
- 28 Gianola D S, Petegem S V, Legros M et al. *Acta Materialia*[J], 2006, 54(8): 2253
- 29 Xu W W, Dávila L P. *Materials Science and Engineering A*[J], 2017, 692: 90

- 30 Honeycutt J D, Andersen H C. *Journal of Physical Chemistry*[J], 1987, 91(19): 4950
- 31 Plimpton S J. *Journal of Computational Physics*[J], 1995, 117(1): 1
- 32 Hirel P. *Computer Physics Communications*[J], 2015, 197: 212
- 33 Voronoi G. *Journal Für Die Reine Und Angewand Mathematik* [J], 1908, 1908(133): 97
- 34 Stukowski A. *Modelling and Simulation in Materials Science and Engineering*[J], 2010, 18(1): 15 012
- 35 Li J. *Modelling and Simulation in Materials Science and Engineering*[J], 2003, 11(2): 173
- 36 Nosé S. *The Journal of Chemical Physics*[J], 1984, 81(1): 511
- 37 Hoover W G. *Physical Review A*[J], 1985, 31(3): 1695
- 38 Zope R R, Mishin Y. *Physical Review B*[J], 2003, 68(2): 24 102
- 39 Hall E O. *Proceedings of the Physical Society Section: Section B* [J], 1951, 643(9): 747
- 40 Petch N J. *Acta Metallurgica*[J], 1986, 34(7): 1387
- 41 Lu K, Sui M L. *Scripta Metall Mater*[J], 1993, 28(12): 1465
- 42 Blum W, Li Y J, Chen J et al. *International Journal of Materials Research*[J], 2006; 97(12): 1661
- 43 Agha A S M. *Journal of Materials Processing Technology*[J], 2009, 209(2): 856
- 44 Swygenhoven H V, Derlet P M, Hasnaoui A. *Physical Review B* [J], 2002, 66(2): 24 101
- 45 Yamakov V, Wolf D, Phillpot S R et al. *Acta Materialia*[J], 2002, 50(20): 5005
- 46 Hull D, Bacon D J. *Introduction to Dislocations*[M]. Amsterdam: Elsevier, 2011
- 47 Lu K. *Nature Reviews Materials*[J], 2016, 1(5): 16 019
- 48 Priester L. *Grain Boundaries and Crystalline Plasticity*[M]. Hoboken: John Wiley & Sons, 2013
- 49 Ding J, Tian Y, Wang L S et al. *Computational Materials Science* [J], 2019, 158: 76
- 50 Song H Y, Li Y L. *Physics Letters A*[J], 2012, 376(4): 529

晶粒尺寸和孪晶界间距对纳米多晶铝合金塑性变形影响的分子动力学模拟研究

任军强^{1,4}, 杨丹¹, 王启², 卢学峰¹, 张旭东³, 薛红涛¹, 汤富领¹, 丁雨田¹

(1. 兰州理工大学 省部共建有色金属先进加工与再利用国家重点实验室, 甘肃 兰州 730050)

(2. 黄淮学院 能源工程学院, 河南 驻马店 463000)

(3. 西安交通大学 网络信息中心, 陕西 西安 710049)

(4. 西安交通大学 金属材料强度国家重点实验室, 陕西 西安 710049)

摘要: 采用分子动力学模拟方法, 分别研究了晶粒尺寸和孪晶密度对纳米多晶铝合金塑性变形的影响。模拟结果表明, 弛豫后的位错密度对纳米多晶Al的微观结构演变和逆Hall-Petch关系产生了重要影响。变形受晶粒大小限制, 在细晶中可形成层错四面体和复杂层错结构, 从而激活了晶界的辅助变形。当孪晶界间距(TBS)较大时, Shockley分位错在晶界处形核并增殖。然而, 随着TBS的减小, 孪晶界成为Shockley分位错的来源。孪晶界上大量的分位错形核会导致孪晶界迁移甚至消失。在塑性变形过程中还观察到形变纳米孪晶。研究结果为开发具有可调节力学性能先进纳米多晶Al提供了理论基础。

关键词: 纳米多晶铝; 晶粒尺寸; 位错; 孪晶; 分子动力学

作者简介: 任军强, 男, 1979年生, 博士, 副研究员, 兰州理工大学材料科学与工程学院省部共建有色金属先进加工与再利用国家重点实验室, 甘肃 兰州 730050, 电话: 0931-2976688, E-mail: renjq@lut.edu.cn